Ref. TH. 853

HADRONIC MATTER NEAR THE BOILING POINT

R. Hagedorn

CERN - Geneva

ABSTRACT

Hadron collisions above ~ 10 GeV/c primary laboratory momentum show an interesting global aspect (i.e., when averaged over all final channels): they can be described as a superposition of a rather special form of thermodynamics and of the kinematics of collective motions in the forward-backward direction. The thermodynamical behaviour is similar to that of boiling; the boiling temperature T_0 is not exactly known but near to 160 MeV; its value and the whole thermodynamic behaviour of hadronic matter follows uniquely from the hadronic mass spectrum. Namely, in this model, as a consequence of a kind of asymptotic bootstrap involving all hadrons, the mass spectrum of hadrons turns out to grow necessarily like $\exp(m/T_0)$ where T_0 is the highest possible temperature (boiling point of hadronic matter).

Global aspects of hadron collisions from ~ 10 GeV/c up to the highest cosmic ray primary momenta ($>10^5$ GeV/c) namely: production rates, differential momentum spectra of secondaries, transverse momentum distributions, etc., agree well with the calculations based on this model. The known part of the hadronic mass spectrum does indeed grow exponentially and the mean transverse momenta of pions produced between 10 and 10^5 GeV/c primary momentum stay very near but always below that value which would correspond to $T = 160$ MeV. The picture which emerges is then:

* there seems to exist a highest temperature (or boiling point of hadronic matter) $T_0 \approx 160$ MeV;

* hadronic matter in collisions above some ten GeV/c primary momentum is in a state where all hadrons melt by way of a universal hadronic bootstrap, into "boiling hadronic matter" in which strong collective motions in the direction of the collision axis coexist with local thermodynamical equilibrium.

67/1384/5 - TH. 853

27 November 1967

1. INTRODUCTION

1.1 Recommendation

Read the abstract.

1.2 Nature of this paper

This is an extremely condensed resumé of three papers [1]: "Statistical Thermodynamics of Strong Interactions at High Energies I, II [*], III" and a fourth one [2] "On the Hadronic Mass Spectrum". I cannot enter here into any details, nor derive any formula but only give a description in words and quote results. The qualitative language to which I am thus forced will unavoidably cause misinterpretations. I humbly ask the reader of this paper, to consult the four above mentioned papers before he utters his final verdict.

We display the material as follows: part 2 describes the thermodynamic aspects, part 3 the kinematics and the parameters, part 4 presents the results and compares them to experiments, part 5 discusses predictions and proposes measurements.

Units: $\hbar = c = k$ (Boltzmann's constant) $= 1$.

2. THE THERMODYNAMIC MODEL

2.1 The main structure of the thermodynamical model

In the thermodynamical model we describe highly excited hadronic matter by relativistic quantum statistical thermodynamics, allowing

---

*) The work reported in (II) was done in collaboration with J. Ranft, now at the Rutherford High Energy Laboratory, England.

arbitrary absorption and creation of hadrons and antihadrons of all kinds, including all resonances. As the spectrum of resonances cannot be limited, we take into account all of them, even the not yet discovered ones. That goes as follows: we introduce one common name: "fireballs" for all hadrons and postulate [the feed-back arrow is most important!]:

A fireball is:

→ a statistical equilibrium of an undetermined number of all kinds of fireballs, each of which, in turn, is considered to be ↩ (T)

We presently forget about complications like collective motions and imagine ideal equilibrium (realistic fireballs are discussed below). One writes down the partition function $Z(V,T)$ for a gas consisting of an undetermined number of all kinds of particles (fireballs) which must be labelled: most conveniently by their mass m. In calculating Z one has to sum over all single particle momentum states in a volume V, over all possible numbers of particles (bosons $0\ldots\infty$, fermions $0,1$) and over all possible kinds of particles (hadrons and antihadrons) - the latter is done by introducing the number of hadron states between m and $m+dm$: namely: $\rho(m)dm$. With this (unknown) function $\rho(m)$ the partition function becomes [see (I)]:

$$Z = \exp\left[\int_0^\infty \rho(m)\, F(m,T)\, dm\right] \tag{1.a}$$

with a known function $F(m,T)$. On the other hand, Z can be written (see any book on statistical mechanics)

$$Z = \int_0^\infty \sigma(E)\, e^{-E/T}\, dE \tag{1.b}$$

where $\sigma(E)$ is the number of states between E and $E+dE$ of the fireball considered; as for this fireball $E=m$ (we stay in its rest frame) we can say as well that we have for our "main" fireball $\sigma(m)dm$ states in the mass interval $\{m, dm\}$. Now $\rho(m)$ is the number of hadron states in the interval $\{m, dm\}$ and if our postulate (T) is applied it follows that asymptotically $\rho(m)$ and $\sigma(m)$ must become somehow the same. A detailed discussion [see (I)] reveals that one cannot require more than that

$$\frac{\log \rho(m)}{\log \sigma(m)} \underset{m\to\infty}{\Longrightarrow} 1 \qquad (2) \equiv (T)$$

which says that for $m \to \infty$ the entropy of a fireball is the same function of its mass, as is the entropy of the fireballs of which it is composed; this implies that all fireballs are on an equal footing.

We now equate the two expressions (1.a) and (1.b) and require simultaneously (2) to be valid. It is shown in (I) that $F(m,T)$ falls off asymptotically like $m^{\frac{3}{2}}\exp(-m/T)$ and that therefore

$$Z \Longrightarrow \exp\left[\int_0^\infty m^{3/2}\rho(m)e^{-\frac{m}{T}}dm\right] \Longleftrightarrow \int_0^\infty \sigma(m)e^{-\frac{m}{T}}dm \qquad (1.c)$$

This is consistent with the "bootstrap" requirement (2) if and only if [see (I)]

$$\rho(m) \underset{m\to\infty}{\Longrightarrow} \frac{const.}{m^{5/2}}\, e^{m/T_0} \quad {}^{*)} \qquad (3)$$

---

*) It is not possible to have this $\rho(m)$ cut off somewhere because this would imply two types of essentially different fireballs: one with almost exponentially diverging density of states $\sigma(m)$, the other with asymptotically vanishing density of states $\rho(m)$, and both would contribute and exist on an equal footing; this is either inconsistent or would indicate something shockingly new at very high energies; but so far and up to 10^5 GeV primary energy there is no experimental indication of anything radically new.

As the partition function Z and all thermodynamical quantities derived from it, diverge for $T \geqslant T_0$ [see (1.c)], it follows that T_0 is the highest possible temperature - a kind of "boiling point of hadronic matter" in whose vicinity particle creation becomes so vehement that the temperature cannot increase anymore, no matter how much energy is fed in.

An immediate consequence is a Boltzmann-type momentum distribution [asymptotically $\sim \exp(-p_\perp/T)$] with $T \approx T_0$, but never larger than T_0. This explains why the transversal momentum distribution in high energy jets is nearly energy independent up to at least 10^5 GeV primary energy! For all details and possible deviations see (II).

Back to the mass spectrum: $\rho(m)$ counts each state (spin, etc.) separately and includes antiparticles. If one smoothes out the experimental mass spectrum [3], one obtains our Fig. 1 in which an exponential increase is seen in the region $\lesssim$ 1000 MeV, i.e., in that region where we know almost all resonances. Extrapolating the experimental curve with an expression having the required asymptotic behaviour (3) yields

$$T_0 = 160 \pm 10 \ \text{MeV}$$

and with this value excellent fits (ranging over 10 orders of magnitude) to the momentum spectra and multiplicities in high energy production processes are obtained (see below).

We treat hadrons as self-consistently infinitely composed of all other hadrons - this is what (T) says. If all hadrons are virtually contained in each of them, it is natural to assume that all phase relations between the infinitely many contributing amplitudes wash out and that therefore statistical thermodynamics is adequate to treat this asymptotic bootstrap. Although the technique is unconventional, it is not so far from the usual ones as one might think: a close relation between the mass spectrum and the momentum distribution in multiparticle production seems unavoidable in any theory, and the Gibbs-ensemble description with fixed T somehow introduces off-shell effects because the masses of fireballs present at temperature T extend to ∞ (with exponentially falling weight).

Recently, two papers [4] have been presented which use conventional quantum mechanical techniques to construct infinitely composed, self-consistent hadrons. A variety of different model assumptions were shown to lead to one common behaviour: the form factors fall off asymptotically like $\exp(-\mathrm{const}\sqrt{|t|})$ in complete analogy with our result on momentum spectra. It seems that the sole requirement of self-consistent infinite composedness is sufficient to produce these asymptotically exponential laws for mass spectra, momentum distributions and form factors - at least this is strongly suggested by the fact that the thermodynamical model does not make any other assumption and that in the papers by Stack and Harte this assumption was the only one common to their various models.

In future, one should distinguish the "vicinity of the boiling point of hadronic matter" *) where $T \to T_0$ and $E \to \infty$ and where literally all hadrons merge into each other in one giant bootstrap. It follows from the small value $T_0 \approx 160$ MeV (some 10^{12} °K) that $E \to \infty$ means in this respect E above some 10 GeV [for quantitative relations, see (II)].

---

*) For all details of particle physics one better looks at the "vicinity of the freezing point", so to speak; namely, where most channels are frozen in (maybe artificially by singling out particular ones).

* if a number n of baryons is "brought-in", e.g., in a πp collision $(n = 1)$, then the fact that only states with baryon number $\geq n$ are contained in Z, causes the temperature-energy relation to be slightly altered (see Fig. 2), but its main effect is an automatic renormalization of the momentum spectrum (4) for baryons such that its norm is no longer equal to the unrestricted production rate of particles of mass m [which goes like $\sim \exp(-m/T)$] but is now proportional to the temperature-independent number n of brought-in baryons. In case there is just one "through-going" baryon, the momentum spectrum of through-going nucleons (not that of newly created ones or of pions, etc.) becomes instead of (4):

$$f_N(\varepsilon, T) \longrightarrow \frac{f_N(\varepsilon, T)}{N_B(T)} \tag{6}$$

In this formula

$$N_B(T) \equiv \sum{}^{*} \int f_{N^*}(\varepsilon, T)\, d^3p \tag{7}$$

represents the total number of all baryonic fireballs existing virtually (and without baryon conservation law) at temperature T; the sum $\sum^*$, which goes over all baryon resonances including the nucleon, can be evaluated with the help of the known baryon mass spectrum and its asymptotic extrapolation. Integrating (6) over all momenta and $\sum^*$ summing gives 1 (by definition) <u>no matter what the temperature is</u>.

This automatic renormalization of the spectra of the through-going baryons (and consequently of all their decay products as nucleons, hyperons, kaons and pions) distinguishes them significantly from all other, newly created particles: we shall see that they can be as peripheral as they like; the others cannot, because in a collision the interior is hot and the peripheral regions are cold (see below); for small T a spectrum like (4) vanishes rapidly in contrast to (6).

2.5 The decay chain

The situation described by the partition function Z at temperature T is that of a quantum mechanical mixture with non-diagonal particle numbers and diagonal density matrix in a representation where the basic states are direct product states built of single particle plane wave states in a volume V; all hadrons, including all resonances, are here considered as "particles". That is, the density matrix and/or Z would allow one to calculate the probability (not amplitude! that is the price we pay) to find a state with so and so many fireballs of such and such masses and momenta, if only we could for a moment switch off strong interactions and allow the state to become an asymptotic state.

As we cannot switch off strong interactions, our fireballs decay. They do so, however, according to the same mechanism as the first fireball did. Thus, there is not only a feed-back definition (T) of our system, it will also decay according to this rule. Nevertheless, it is practically impossible to follow the process by a calculation (except, perhaps one of Monte Carlo type), because the "decay chain":

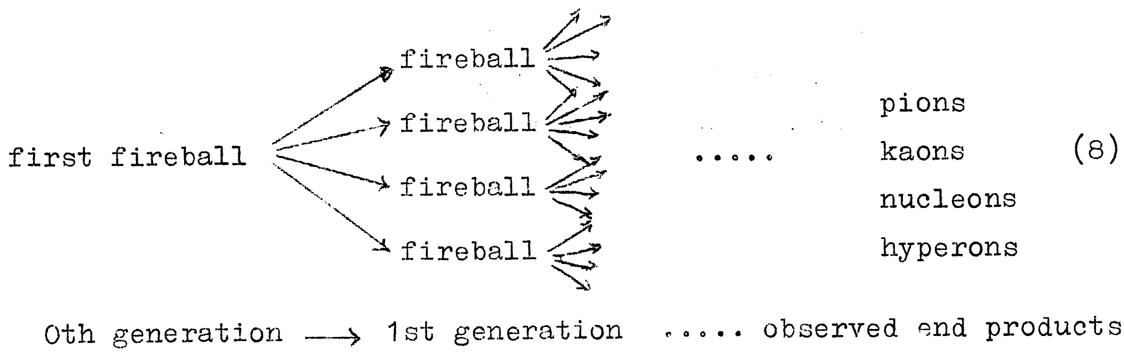

(8)

is too complicated: the ith generation is found from applying to each fireball of the (i-1)th generation the whole theory (each has another mass, temperature, etc.) and a Lorentz transformation from its rest frame to the observers frame and then integrating all this over its velocity spectrum and sum over all such fireballs of the (i-1)th generation, which latter is linked in the same way to the (i-2)nd one, etc., etc., until we end up with the original fireball. Of course, the whole thing, even the number of generations, is itself only a probability distribution and, in the last few steps leading to the observed particles, thermodynamics can no longer be applied as their two - and three-body decays with their selection rules and non-thermodynamic spectra (even δ shaped) dominate.

Thus, the partition function only yields the momentum spectra and all that for the first generation; however, we hope that all the rest will average out, so that the final particles will almost appear as if they had been created in the first generation. The effect of interlacing decays and Lorentz transformations would then only be to smear out the spectra so that they look still thermodynamic but must be calculated with an effective temperature T_{eff} which might be somewhat larger than the true temperature of the first fireball. One only should single out those particles which jump over all generations and reach the final state directly from the first generation via a two-body decay like $N^* \rightarrow N + \pi$: through the one single two-body decay their spectrum would be strongly distorted and no longer look like a first generation spectrum.

These hopes came indeed true. A model calculation [with Lorentz transformations (weighed by the spectra of the first generation) and all that] down to the second generation showed that these spectra are roughly thermodynamic with $T_{eff} \gtrsim T$ and that two-body decays must be treated apart. Thus, the rule of approximation is:

treat final particles as if they had come from the first generation, but allow for an effective temperature $T_{eff} \gtrsim T$ to roughly account for all the neglected kinematics of the decay chain; treat two-body decays apart. (9)

Improvements are possible, straightforward and tedious: go down by exact iteration to the second generation, take two - and three-body decay apart, and so on.

Our experience shows that this is not necessary with the present experimental precision; the above first approximation yields excellent results.

3. KINEMATICS ADDED: REALISTIC DESCRIPTION OF A COLLISION

3.1. Velocity distribution

At some instant during a proton-proton collision the situation will look like this:

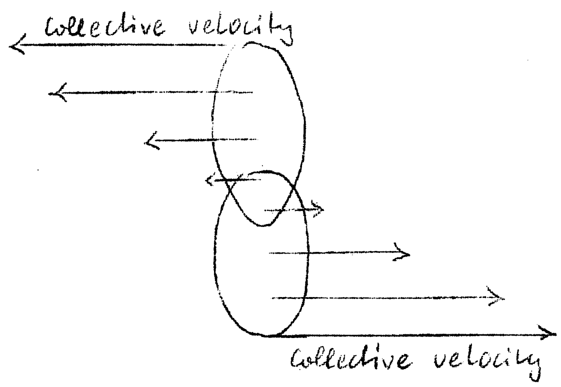

there will be strong collective motions in the forward-backward direction with velocities ranging from zero to the initial velocity v_0 of the protons. This velocity distribution will vary considerably during the collision time $\Delta t \approx 2r/\gamma_0$, it will strongly depend on the impact parameter and of which particles collide (symmetric in pp collisions, asymmetric in πp etc.) and it will not even be a unique space-time function because the uncertainty relation requires that in a small volume element there is a whole velocity spectrum.

We thus define a velocity weight function, which collects (over the whole history of a collision, over the whole interaction volume and in the average over all impact parameters) all contributions to a given velocity and attaches a weight to this velocity.

As variable we do not use the velocity itself, which is always nearly equal to 1 and thus not suitable, we use the variable

$$\lambda = \mathrm{sgn}(v) \cdot \frac{\gamma - 1}{\gamma_0 - 1} \quad ; \quad \gamma = (1 - v^2)^{-1/2} \tag{10}$$

and call it "velocity" although it measures velocity in terms of the ratio (kinetic energy density γ-1)/(initial kinetic energy density γ_0-1). Thus, always $-1 \leq \lambda \leq 1$.

We define the weight function $F(\lambda)$ and normalize it to 1 (separately in $0 \leq \lambda \leq 1$ and in $-1 \leq \lambda < 0$).

This velocity weight function describes then, so we hope, an essentially geometrical situation and thus should depend only little on the primary energy which is hidden in the mapping of the actual velocity range $-v_0 \leq v \leq v_0$ onto the interval $-1 \leq \lambda \leq 1$.

We consider only velocities in the forward-backward direction: transversal collective motions (turbulence) are completely absent or at least so small that they are negligible compared to the heat motion, which itself is small ($T \lesssim 160$ MeV). The transversal momentum distribution in collisions with up to and above 10^5 GeV primary energy proves this beyond any doubt for pions and leave only little doubt as far as through-going baryons are concerned.

Our calculations show that for pp collisions with primary momentum p_0 between 12 and 30 GeV/c two energy independent velocity weight functions are sufficient to describe all spectra [Fig. 3 shows $F(\lambda)$ and $F_0(\lambda)$]:

* one function $F(\lambda)$ for all newly created particles (pions, kaons, antinucleons, etc.);

* one function $F_0(\lambda)$ for the through-going baryons, which need not be created.

3.2 Temperature-velocity relation

We have (numerically) calculated the temperature as function of the energy density $\mathcal{E}$ (see 2.2 above). We now postulate (A for adiabatic):

> the kinetic energy of the incoming particles, which is lost during the deceleration process leading to the velocity λ, is adiabatically transformed into heat. (A)

Indeed, the only way in which heat can escape is by radiating off particles; and this only starts when the temperature comes to reach the order of T_o, because T_o is not much different from the pion mass and the production rates go all like $\exp(-m/T)$. Thus, the smallness of T_o guarantees that the annihilated kinetic energy is nearly adiabatically transformed into heat (if T_o were hundred GeV, this would be different). Once (A) is accepted, it is easy to see that the energy density corresponding to adiabatic deceleration from velocity 1 to velocity $|\lambda|$ is given by

$$\varepsilon(\gamma_o, \lambda) = \varepsilon_o \gamma_o \left[1 + |\lambda| \cdot (\gamma_o - 1)\right]^{-1}$$

where $\varepsilon_o = m_p/V$ is the energy density (in the rest frame) before deceleration transforms collective kinetic energy into heat.

Thus, with $T = T(\varepsilon)$ and $\varepsilon = \varepsilon(\gamma_o, \lambda)$, we have now available the function

$$T = T(\gamma_o, \lambda) = \left\{ \begin{array}{l} \text{numerically tabulated function of the velocity} \\ \lambda \text{ and of the primary energy } \gamma_o. \end{array} \right\}$$

It is now clear why - roughly speaking - the interior of the interaction region is hot and the peripheral parts are cold.

3.3 Lorentz transformation

For a given velocity λ, there is a rest frame (we call it λ frame) where the temperature $T(\gamma_o, \lambda)$ is uniquely determined, and where the only motion is heat motion, the collective motion being transformed away.

Thus, in the λ frame our thermodynamics of Section 2 rules undisturbed by collective motions. The temperature is $T(\gamma_0, \lambda)$ and the momentum spectra of all particles, correctly normalized to the total production rate, can be calculated there. The more λ tends to ± 1 (that is: the more peripheral the contributing regions are) the more important becomes the difference between through-going and newly created particles.

The λ frame contributes with weights $F(\lambda)$ and $F_0(\lambda)$ respectively to the over-all yield.

It remains to transform the isotropic momentum spectra from the λ frame to the centre-of-momentum (c.m.) frame by a Lorentz transformation $L(\lambda)$ which is uniquely defined as it goes in the forward or backward direction according to sign and magnitude of λ. This Lorentz transformation is responsible for almost the whole longitudinal momentum, in particular for $\lambda \to 1$.

Our model is - expressed in familiar terms - a continuous superposition of an infinity of fireballs, each characterized by a "velocity" λ and decaying according to our thermodynamics at temperature $T(\lambda)$.

3.4 Representative isobars

We mentioned above that the decay chain with its complicated interplay of kinematics and thermodynamics can be simulated by a simple first generation calculation, allowing for an effective temperature $T_{eff} = \tau \cdot T(\lambda)$; $\tau \gtrsim 1$.

This works very well except for two-body decay; and there the most exhibited two-body decays are those of through-going baryons, which themselves have already a rather particular spectrum due to the fact that they can be very peripheral. Thus, the decays $N^* \to N+\pi$ and/or $\to Y+K$ must be treated apart. Instead of summing this contribution over all baryon resonances, we took some representative ones (the few lowest) and allowed them to choose their own weight $A(N^*)$: with the result that these weight factors A increased exponentially with $m(N^*)$, roughly as if we had calculated these A's from the baryon mass spectrum. We consider this as a sign of consistency.

If an N^* with thermodynamic spectrum in the λ frame makes a two-body decay, then the spectrum $f^*_{i,N^*}(\varepsilon',T)$ of the decay products $(i = \pi, N, K, Y)$ can be analytically calculated in the λ frame and Lorentz transformed to the c.m. frame. This settles the two-body decay.

3.5 Various contributions to the observable spectrum of a particle; graphical representation

On the basis of all the foregoing discussions we can now graphically symbolize various contributions to particle spectra, e.g., for a newly created "i":

$$\bigcirc\!\!\longrightarrow i \quad \equiv F(\lambda)\, L(\lambda)\, f_i(\varepsilon', T(\lambda)) \qquad (11)$$

with obvious interpretation: $f_i(\varepsilon',T(\lambda))$ is the isotropic thermodynamical spectrum of particle "i" in the λ frame, $L(\lambda)$ transforms it to the c.m. frame and $F(\lambda)$ says with which weight this contributes. Another example:

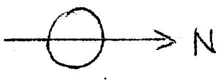

$$\equiv \frac{F_0(\lambda)}{N_B(\lambda)} L(\lambda) f_N(\varepsilon',T) \tag{12}$$

This is a "through-going" nucleon; the main difference with regard to (11) is the factor $1/N_B(\lambda)$ which can be thought of "absorbing the incoming nucleon", which, then is freely re-created by $f_N(\varepsilon',T)$. Next, consider

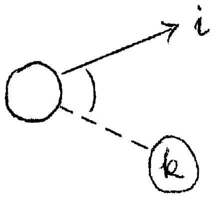

$$\equiv \left[F(\lambda)\right]^2 \cdot N_k(\lambda) \cdot L(\lambda) \cdot f_i(\varepsilon',T) \tag{13}$$

Here, (i,k) pair creation is symbolized; $F(\lambda)$ appears squared; $N_k(\lambda)$ is defined similar to $N_B(\lambda)$; but, here, it counts all the particles of the family "k" which must delegate one of its members to the birth of particle "i". Formula (13) is easily derived from Eq. (5) once it is assumed that such conservation laws as strangeness and baryon number act locally, i.e., that "i" and "k" were born nearly at the same place and thus with almost equal velocity λ [otherwise (13) would contain a free correlation function]. We checked this assumption in various ways and found it valid (see Fig. 4) in the cases where experimental material was available [compare (II)]. Last example :

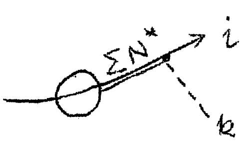

$$\equiv \frac{F_0(\lambda)}{N_B(\lambda)} \cdot L(\lambda) \cdot \sum A_{N^*} f^*_{i,N^*}(\varepsilon',T) \tag{14}$$

which gives the contribution of isobar decay (through-going isobars) to the spectrum of particle "i".

Rules for constructing further such graphs (which have of course nothing to do with Feynmann graphs) have been given in (II). Note that the drawn lines are only those which contribute to the spectrum under consideration and/or are required by conservation laws. The presence of an undetermined number of other particles is always implied in a thermodynamic spectrum and everything is averaged over all channels.

3.6 The actual production spectra

Without going into any details [for which (II) must be consulted], we list a few total c.m. spectra which are obtained by adding contributions like (11) through (14) and integrating over λ from -1 to +1. The dependence on the primary energy γ_o is hidden in the variable λ. One obtains (we neglect some less important graphs and other details in this example)

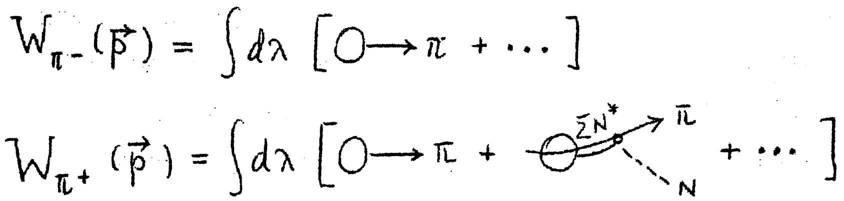

(15a)

(15b)

furthermore,

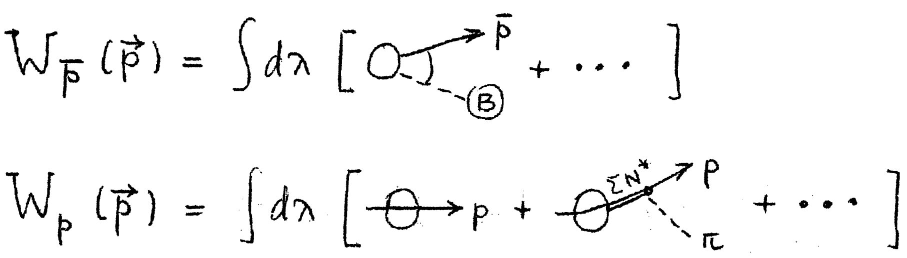

(16a)

(16b)

$$W_{K^-}(\vec{p}) = \int d\lambda \, [$$ 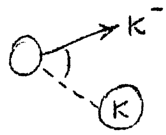 $$+ \dots] \qquad (17a)$$

$$\bar{W}_K(\vec{p}) = \int d\lambda \, [$$ 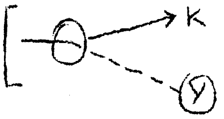 $$+ \dots] \qquad (17b)$$

We have selected examples which show clearly that the spectra of π^- and π^+ or of $\bar{p}$ and p or of K^- and K^+ will be very different: all those where main contributions come from through-going particles are much stronger forward-backward peaked (or: more peripheral) than the others.

The above spectra are c.m. spectra; similar ones can be written down for all particles, also neutrals, if one uses some approximate relations calculable from Clebsch-Gordan algebra of charge ratios. Such a charge analysis also shows that isobar decay contributes much more to π^+ than to π^-, hence the difference between (15a) and (15b).

Once all spectra have been written down - assuming the weight functions $F(\lambda)$ and $F_0(\lambda)$ are fixed - the mean energies $\langle \varepsilon_i \rangle$ of all particles can be calculated and the conservation of the total c.m. energy is required: this yields the absolute normalization of the spectra, which then are completely known.

3.7 Parametrization

Except for parameters which are more or less known a priori, as, for instance, the interaction volume $V \approx (4\pi/3)m_{\pi}^{-3}$ or the ratio $\tau = T_{eff}/T(\lambda) \approx 1$ - except for such uninteresting and almost predetermined parameters, only the two weight functions $F(\lambda)$ and $F_0(\lambda)$ are completely unknown and not calculable from the model. They have to be determined by fitting expressions like (15) through (17) to the experiment. It turned out that simple forms worked very well:

$$F(\lambda) = \frac{1}{N} (1-\lambda) e^{-a\lambda} \tag{18}$$

$$F_0(\lambda) = \frac{1}{N_0} \left[(1-\lambda) e^{-b\lambda} + d\lambda\, e^{-c(1-\lambda)} \right] \tag{19}$$

where N and N_0 respectively normalize the functions to 1 over $0 \leq |\lambda| \leq 1$.

The surprising result of our analysis of experimental data of pp collisions with primary lab. momenta from 12 to 30 GeV/c [5] was that

one set of four energy independent parameters values, the same for all particles, namely:

$$\begin{aligned} a &= 5.6 \\ b &= 20.8 \\ c &= 2.4 \\ d &= 7.1 \end{aligned} \tag{20}$$

was sufficient to reproduce all measured spectra in this energy region with tolerable to excellent agreement, except for some slight discrepancy at very low secondary c.m. momenta. This discrepancy can be easily removed by introducing a few more graphs and one more parameter in the weight functions; before doing so, more experimental data should be awaited.

4. COMPARISON TO EXPERIMENTS

Figures 4 through 8 speak for themselves. Many more such figures could be produced.

The mentioned discrepancy at low c.m. momenta is displayed in Fig. 9 where unusual variables ($p_\perp$ and $p_\parallel$) are used. Note that this is the worst discrepancy we met.

Not only the spectra but also some integral quantities as multiplicities, mean transverse momenta, etc., were cross-checked with experiments; for this, see Figs. 10-14.

In (III) we calculated production rates for heavy pairs:

	$\bar{K}$	$\bar{p}$	$\bar{d}$
Theory	0.07	0.002	1×10^{-9}
Experiment	0.096	0.002	"order of 10^{-9}"

so that from pions to antideuterons the multiplicities cover a range of about ten orders of magnitude and come out rather well. [The conclusions drawn in (III) with regard to quark production rates are discouraging: if quarks have a mass > about $4m_p$, they might never be seen, even if they exist.]

We find that at 30 GeV/c primary momentum the through-going baryons and their decay products carry away 75% of the total c.m. energy, at $p_o = 300$ GeV/c it is still 67%. Thus, in our model a few particles get automatically most of the energy - a well-known fact of cosmic ray physics ("leading particles").

The mean transverse momentum $\langle p_\perp (p_\parallel) \rangle$ as a function of the longitudinal momentum shows a significantly different behaviour for pions and for protons (Figs. 12 and 13) which is due to their different masses.

5. CONCLUDING REMARKS

Apart from offering a simple and consistent description of global aspects of high-energy hadron collisions, our model is presently the safest basis for predictions of what will happen at energies where measurements are not yet available, i.e., essentially in all collisions with $\gtrsim$ 30 GeV/c (in a near future: $\gtrsim$ 70 GeV/c). As such predictions may have far reaching practical consequences in planning future accelerators, we feel that an effort should be made to make our predictions (we calculated everything for 30, 70, 200 and 300 GeV/c; not yet published) more reliable as they presently are.

The discrepancy between theory and experiment displayed in Fig. 9 can easily be removed, but for this, new measurements of very low secondary momenta at $p_o \gtrsim 30$ GeV/c are necessary. At this energy no measurements *) of secondary $\bar{p}$ and K exist and the data obtained at $\approx$20 GeV/c do not provide a safe basis for extrapolations to several hundred GeV/c.

---

*) on hydrogen targets.

We think therefore that the remaining gaps in the experimental information should be closed and that a complete set of measurements at 70 GeV/c primary momentum (on hydrogen targets) of spectra of $\pi^{\pm}$, $K^{\pm}$, N and $\bar{N}$, including very low secondary momenta, is highly desirable. For details see (II).

Computing programmes (CDC 6600 - SCOPE), written by J. Ranft [6) carrying out the calculations described in this paper (as well as the calculations according to other spectral formulae) are available at CERN on request.

ACKNOWLEDGEMENT

I wish to thank the editors of the Nuovo Cimento for the kind permission to reproduce here small parts of the texts and some of the figures of the papers cited in Refs. 1), 2).

REFERENCES

1) R. Hagedorn, Suppl. Nuovo Cimento 3, 147 (1965) - (I);
R. Hagedorn and J. Ranft, to be submitted to the Nuovo Cimento Suppl., CERN preprint TH. 851 (Nov. 67) - (II);
R. Hagedorn, to be published in Nuovo Cimento Suppl., CERN preprint TH. 751 - (Apr. 1967) - (III).

2) R. Hagedorn, "On the hadronic mass spectrum", to be published in the Nuovo Cimento, CERN preprint TH. 827 (Sept. 67).

3) A.H. Rosenfeld, A. Barbaro-Galtieri, J. Podolsky, L.R. Price, P. Söding, C.G. Wohl, M. Roos and W.J. Willis, Revs.Modern Phys. 39, 1 (1967).

4) J. Stack, "Rapidly decreasing form factors and infinitely composed particles", University of Illinois preprint, June 1967;

J. Harte, "Crossing-symmetric bootstrap and exponentially falling form factors", University of California preprint, August 1967.

5) For detailed references to experimental data see (II).

6) J. Ranft, "Two computer programmes to calculate and plot secondary particle yields according to various formulae", Programme library numbers W129, W130, Internal report PS/6168 (2o Oct. 1967).

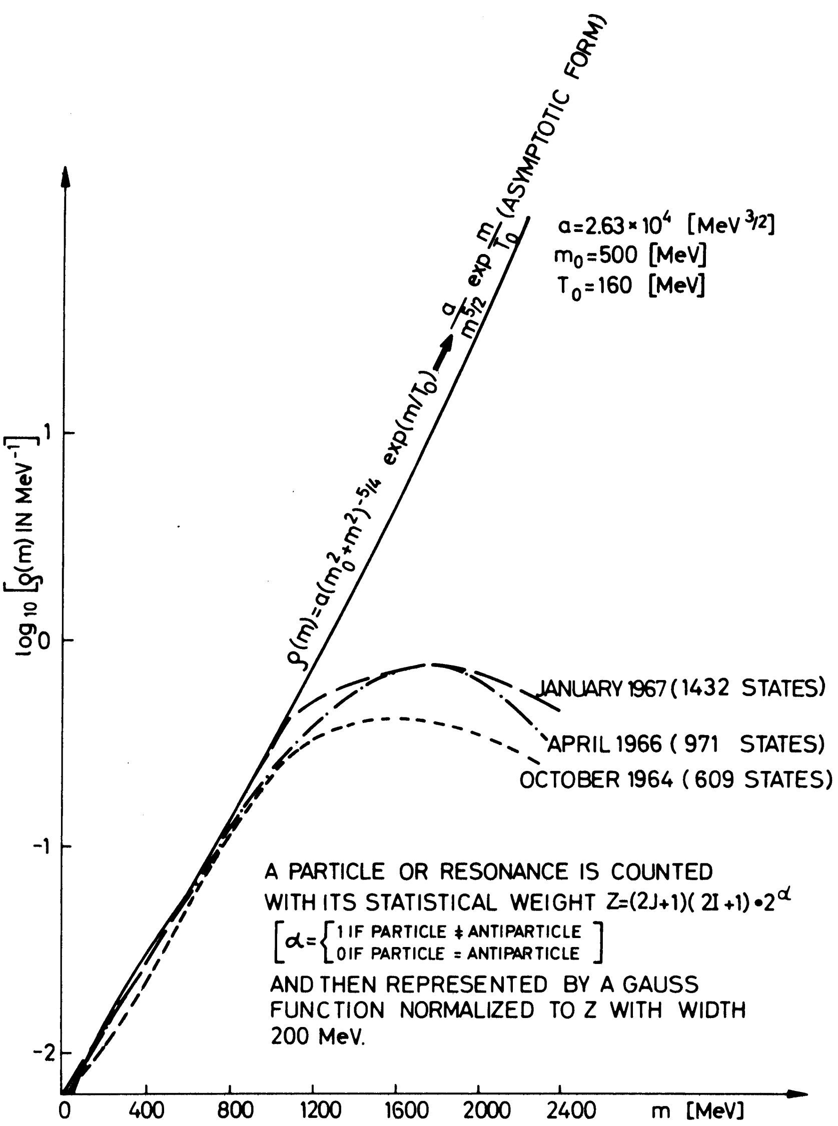

Fig. 1 : The smoothed experimental mass spectrum[3)] as it developed from October 1964 until January 1967 (various dotted lines) and the function $\rho(m) = a(m_0^2 + m^2)^{-5/4} \exp(m/T_0)$ which has the asymptotic form required by the thermodynamical model.

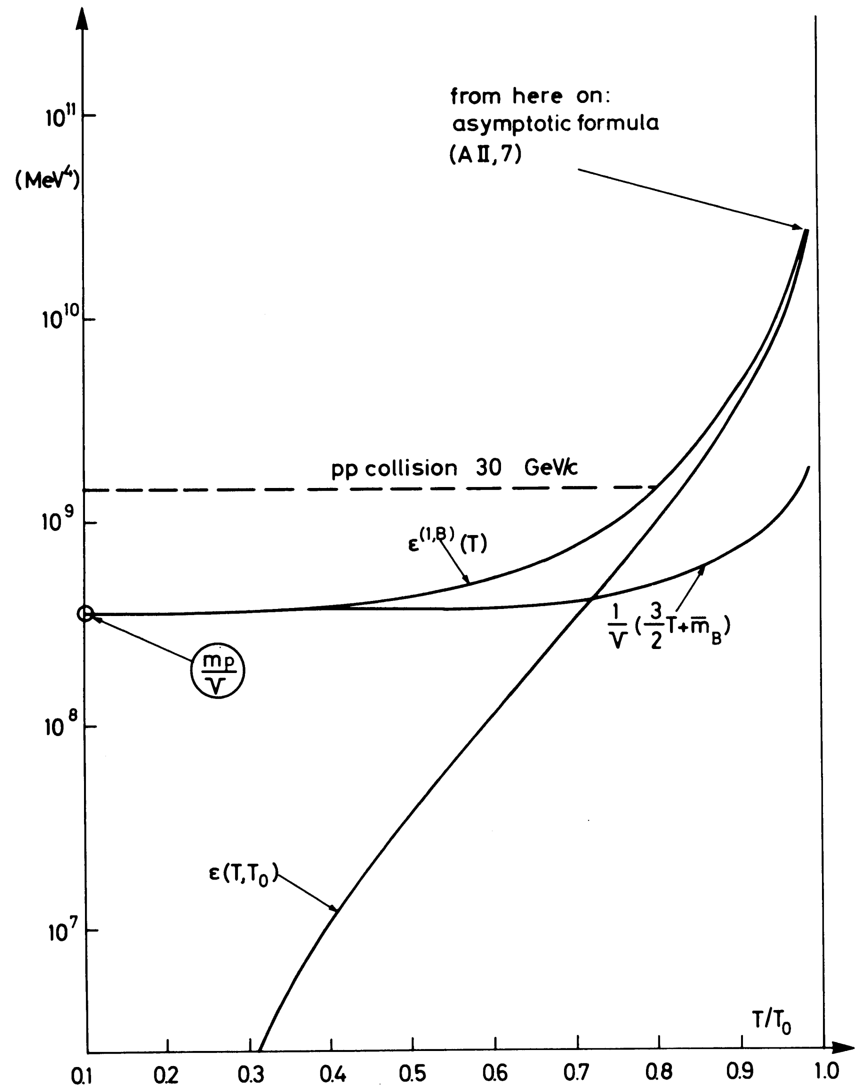

Fig. 2 : The relation between temperature and energy density as calculated from the partition function (paper II) for $T_0 = 160$ MeV:

$\epsilon(T,T_0)$ = energy density inside an "empty" black box of temperature T;

$\frac{1}{V}\left(\frac{3}{2}T + \bar{m}_B\right)$ = energy density (kinetic + mass + excitation) of a brought-in and conserved baryon in the black box at T;

$\epsilon^{(1,B)}(T)$ = total energy density in the black box at T when one brought-in baryon is present (sum of the first two densities).

["asymptotic formula (AII.7)" refers to paper (II).]

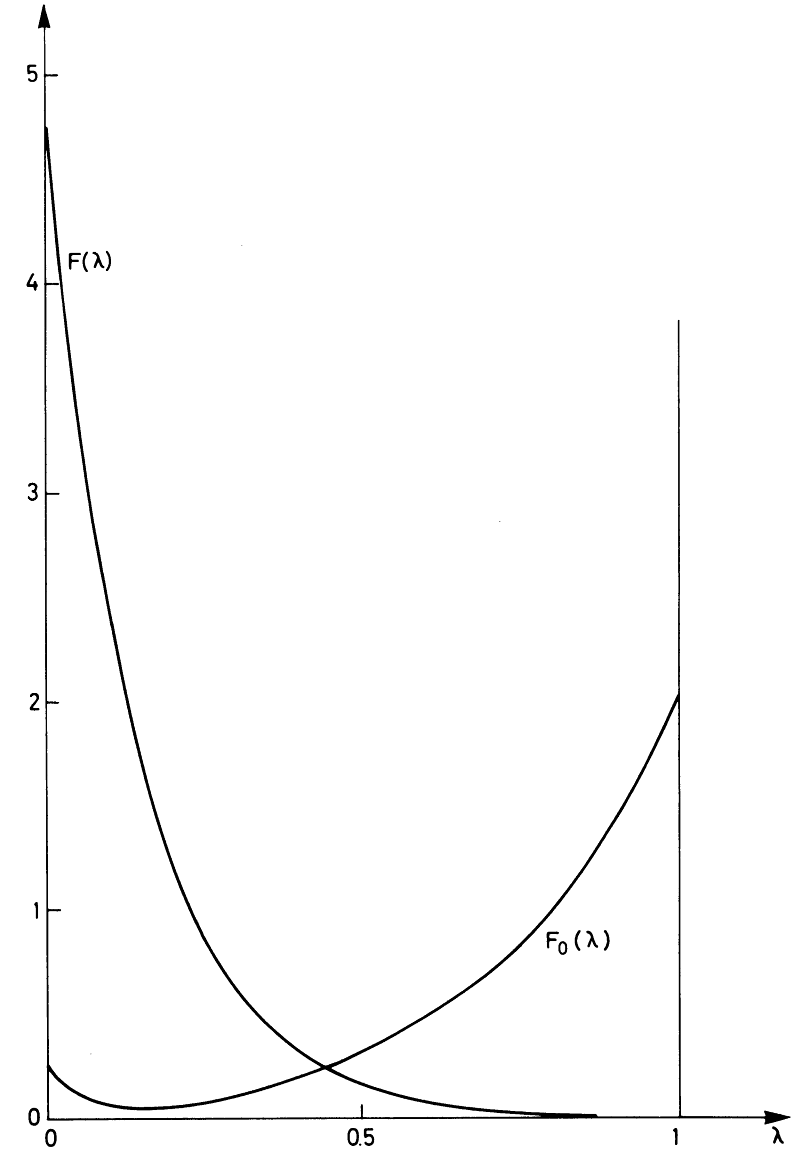

Fig. 3 : The velocity weight functions $F(\lambda)$ and $F_0(\lambda)$; $|\lambda| = (\gamma - 1)/(\gamma_0 - 1)$. $F(\lambda)$ is for newly created particles and puts most weight on small velocities (central parts). $F_0(\lambda)$ belongs to "through-going" baryons and emphasizes the larger velocities (peripherical parts). With these two functions all spectra between 12 and 30 GeV are fitted (i.e. the four "essential parameters a, b, c, d" determining the shape of these functions, have each a fixed numerical value which remains the same for all spectra and through the whole range of primary energy).

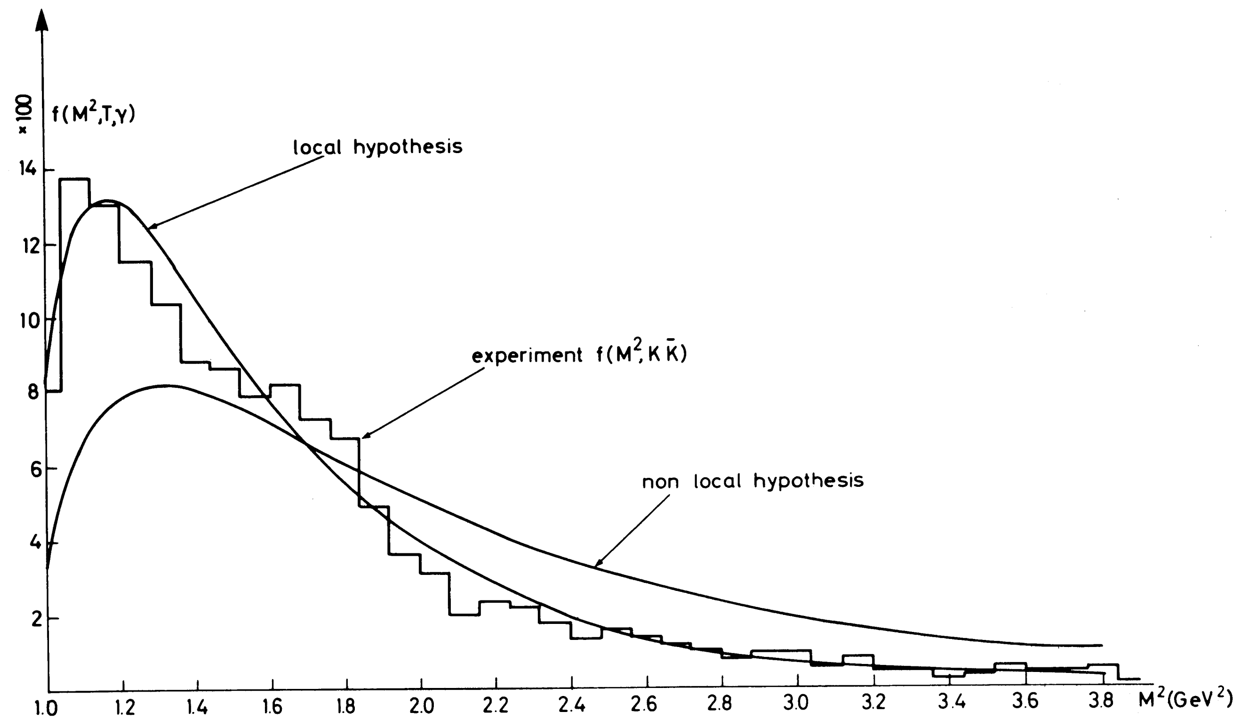

Fig. 4 : Experimental mass distribution $f(M^2)$ of $K\bar{K}$ pairs from $p\bar{p}$ annihilation at 1.2 GeV/c [5] compared to two thermodynamical distributions obtained under the assumptions that K and $\bar{K}$ originate from the same or from distant locations, respectively. For details, see paper (II).

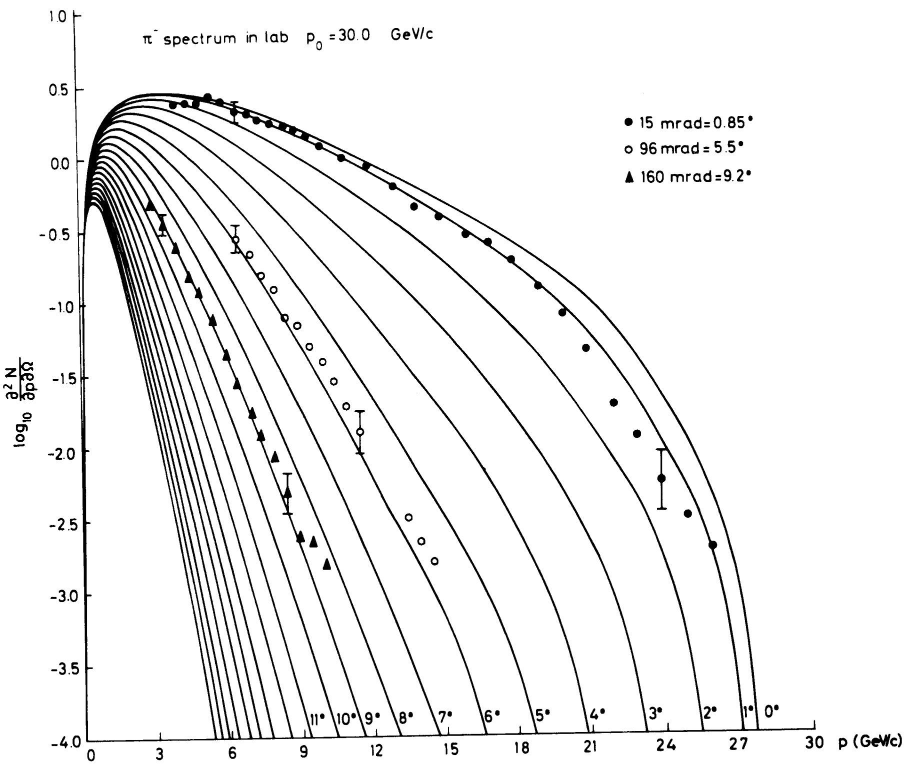

Fig. 5 : The π^- lab. spectrum (p_o = 30 GeV/c) [5] with some typical experimental errors drawn in. Our curves result from a common "one essential parameter" - fit together with K^- and $\bar{p}$ (see Fig. 7).

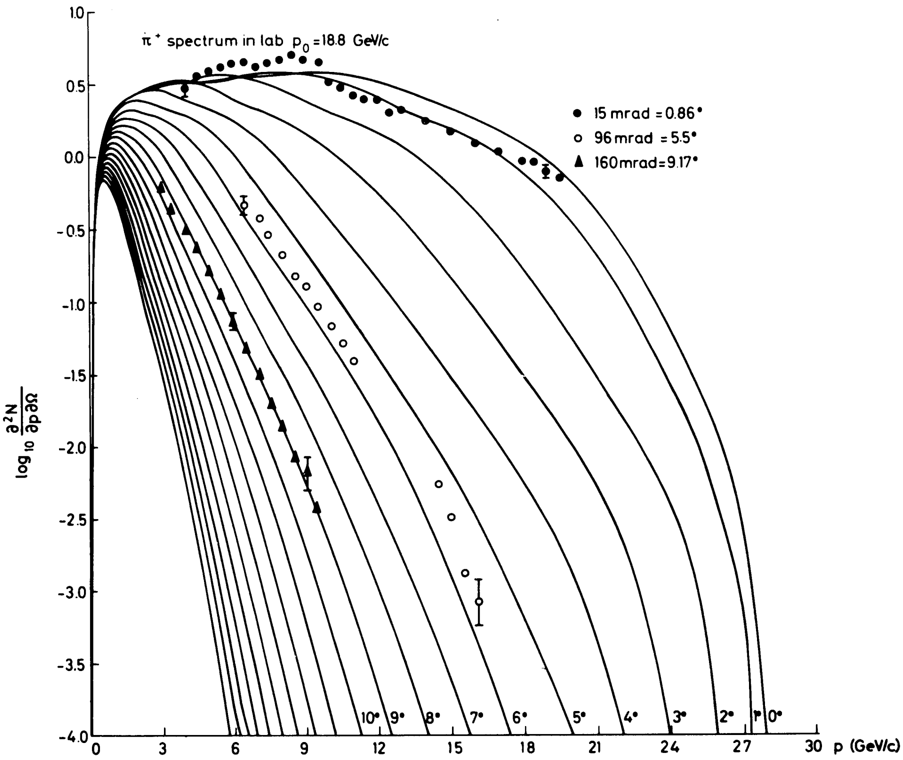

Fig. 6 : π^+ lab. spectrum (p_0 = 30 GeV/c) [5] with some typical errors drawn. Our curves result from a common fit to p and π^+. (The bump near 9 GeV/c in the 15 mrad experiments is possibly due to an instrumental error.)

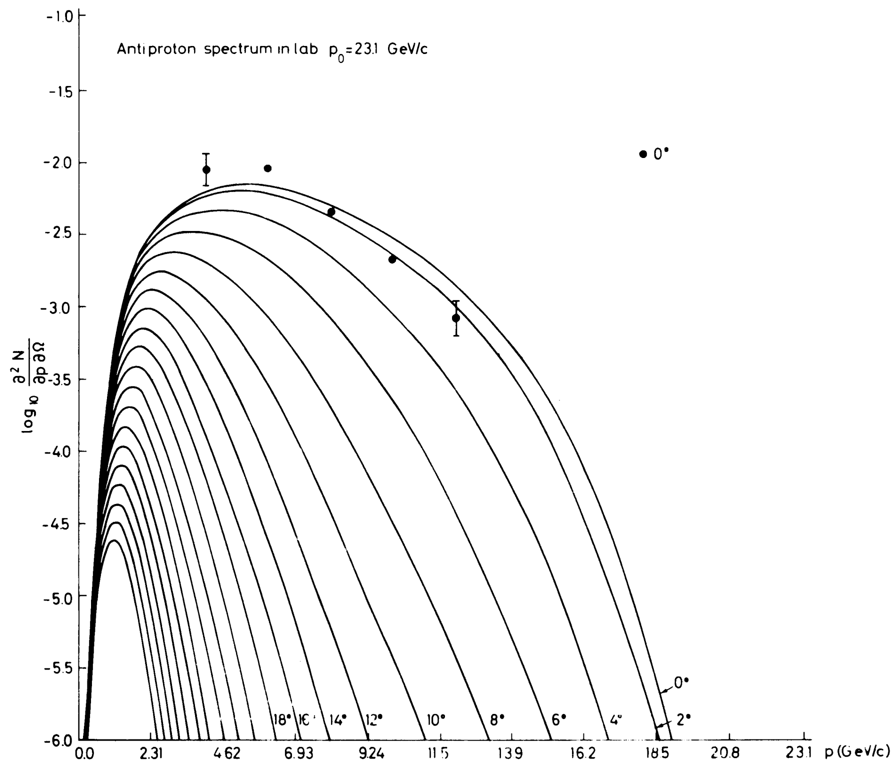

Fig. 7 : $\bar{p}$ lab. spectrum (p_0 = 23.1 GeV/c) [5] with typical errors drawn. Our curves are the result of the common "one essential parameter" - fit to π^-, K^-, and $\bar{p}$ (cf. Fig. 5). Compare these newly created antiprotons to the through-going protons (Fig. 8)! The odd values of p are due to on-line plotting of the curves.

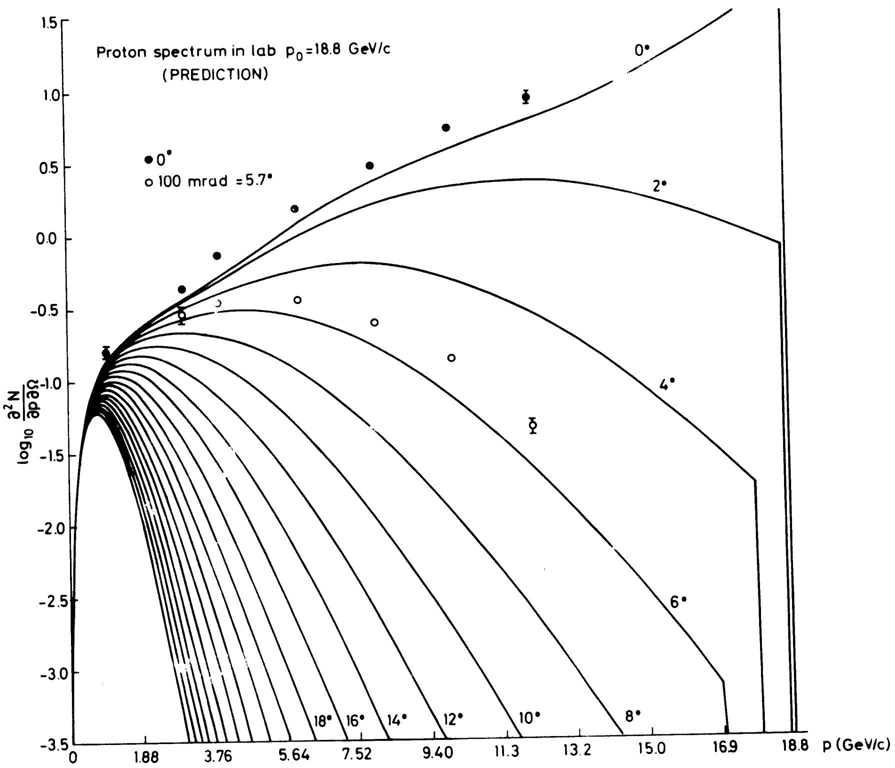

Fig. 8 : p lab. spectrum (p_0 = 18.8 GeV/c) [5] with some typical errors drawn. Our curves are pure predictions, using the parameter values obtained at other energies. Compare these through-going protons with the newly created anti-protons (Fig. 7)! The odd p values are due to on-line plotting of the curves.

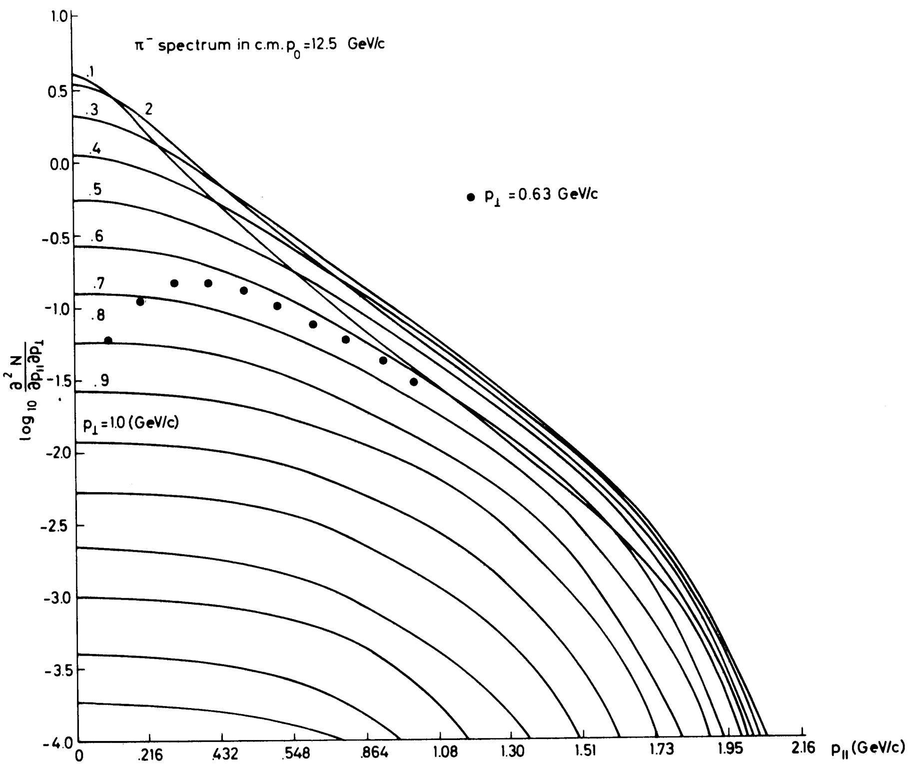

Fig. 9 : The c.m. differential spectrum of π^- plotted as function of $p_{\parallel}$ with $p_{\perp}$ labelling the curves: pure prediction. Note the disagreement below 300 MeV/c (removable by a refinement of the model). The odd values of $p_{\parallel}$ are due to on-line plotting of the curves.

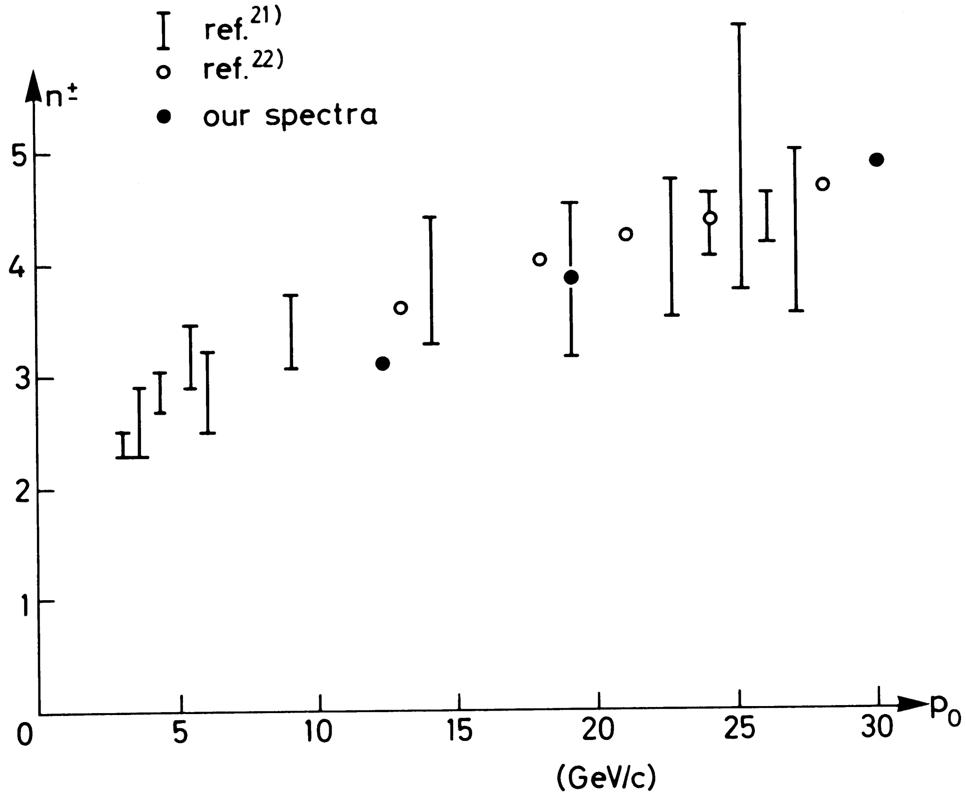

Fig. 10 : Comparison of the total charged multiplicities (obtained by integrating our spectra) with experimental values [for the quoted references 21) and 22) see paper (II)].

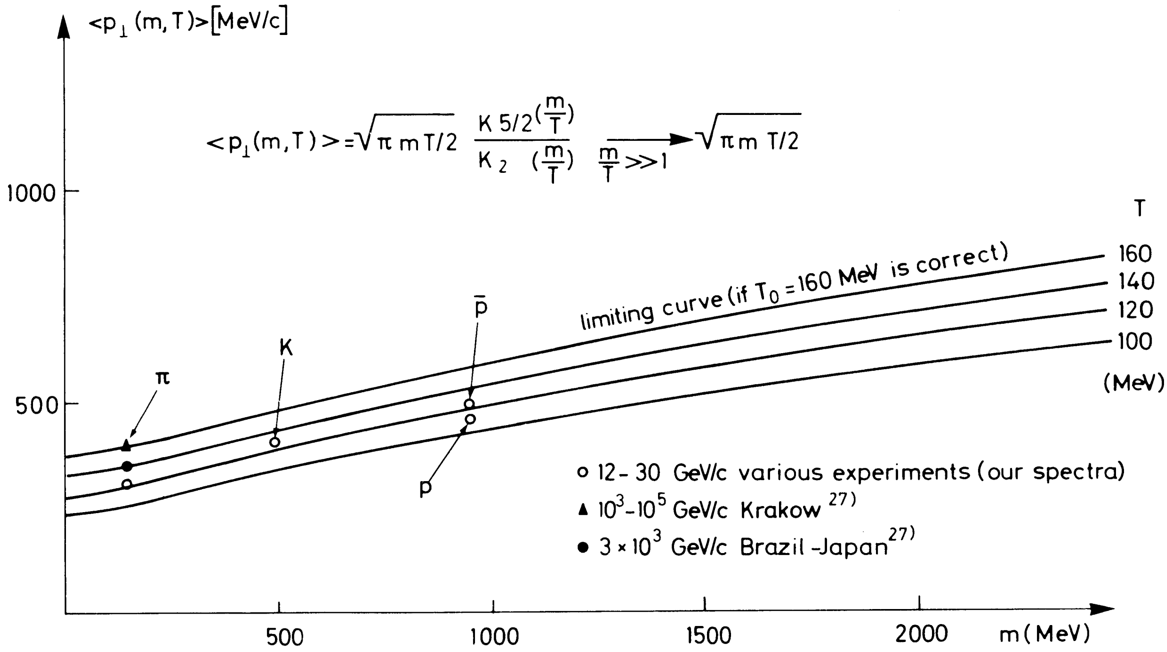

Fig. 11 : The mean transverse momentum $\langle p_\perp \rangle$ as function of the mass of the particle and the temperature of the place from where it is emitted. T may be considered roughly as the mean value of the temperature over the interaction region. Our experimental values (12-30 GeV/c) should lie near $T \approx 128$ MeV; antiprotons come from the hot central regions, protons also from the cold peripherical regions of the collision, hence $T_{\bar{p}} > T_p$. Some cosmic-ray data coming from very high primary energy have been drawn in. They approach the limiting curve (T = 160 MeV) [for the quoted reference 27) see paper (II)].

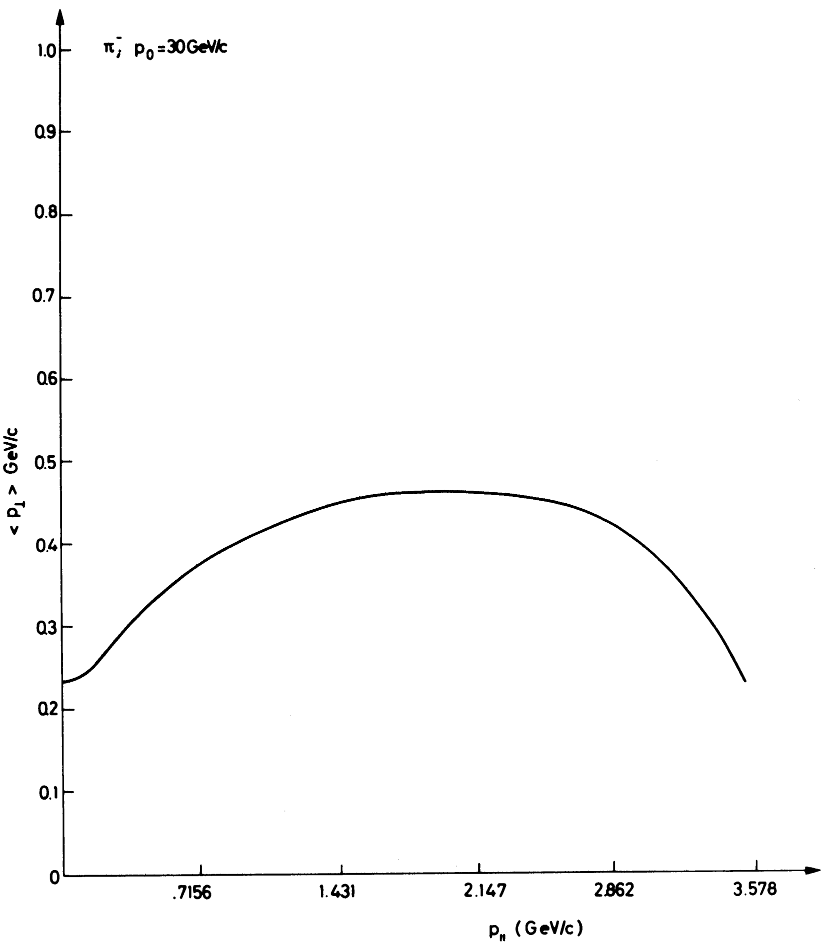

Fig. 12 : Mean transverse momentum of pions $\langle p_\perp(p_{\parallel})\rangle$ as a function of their longitudinal momentum in the c.m. frame. Note the decrease of $\langle p_\perp \rangle$ towards small $p_{\parallel}$, which is absent in the corresponding curve for protons (cf. Fig. 13); the effect is due to the smallness of the pion mass. The curve is obtained numerically from our π^- c.m. spectra (p_0 = 30 GeV/c).

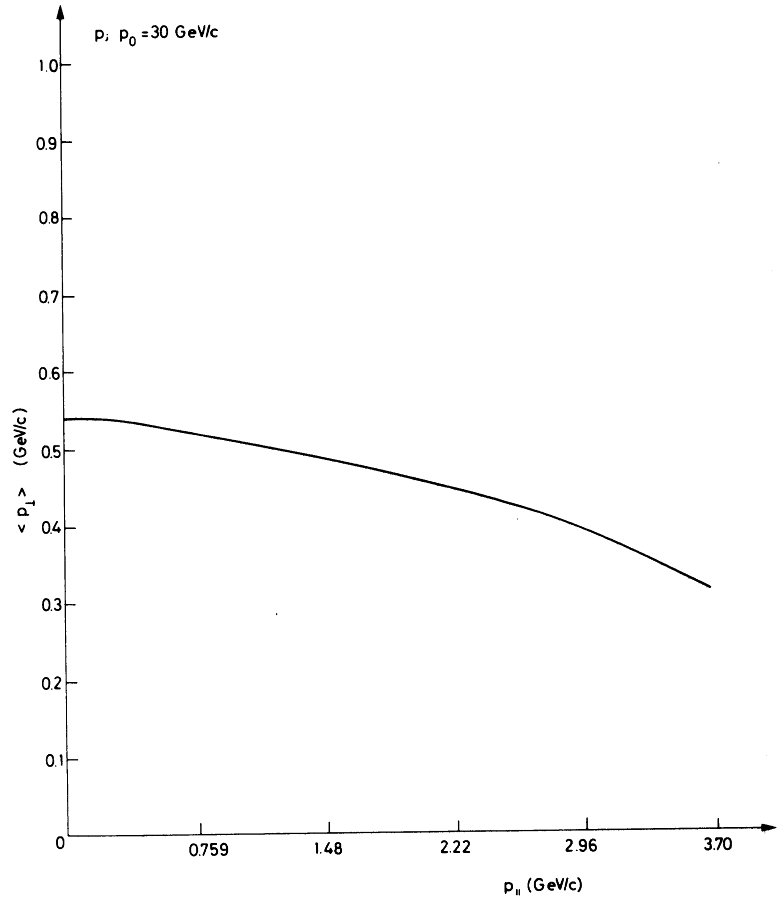

Fig. 13 : Mean transverse momentum of protons $\langle p_\perp(p_{\parallel})\rangle$ as a function of their longitudinal c.m. momentum $p_{\parallel}$. Note the monotonous increase towards small $p_{\parallel}$ in contradistinction to the decrease in the corresponding pion curve (cf. Fig. 12); the difference in behaviour is due to the difference of the masses of π and p. The curve is obtained by numerical integration of our c.m. spectra (p_0 = 30 GeV/c).